Neuroimaging

Nonparenchymal fluid is the source of increased mean diffusivity in preclinical Alzheimer's disease

Farshid Sepehrband[a,*], Ryan P. Cabeen[a], Giuseppe Barisano[a,b], Nasim Sheikh-Bahaei[c,d], Jeiran Choupan[a,e], Meng Law[a,f], Arthur W. Toga[a], for the Alzheimer's Disease Neuroimaging Initiative

[a]Laboratory of Neuro Imaging, USC Stevens Neuroimaging and Informatics Institute, Keck School of Medicine, University of Southern California, Los Angeles, CA, USA
[b]Neuroscience Graduate Program, University of Southern California, Los Angeles, CA, USA
[c]Department of Radiology, Keck School of Medicine, University of Southern California, Los Angeles, CA, USA
[d]Department of Neurology, Keck School of Medicine, University of Southern California, Los Angeles, CA, USA
[e]Department of Psychology, University of Southern California, Los Angeles, CA, USA
[f]Radiology and Nuclear Medicine, Alfred Health, Melbourne, Australia

Abstract

Introduction: Although increased mean diffusivity of the white matter has been repeatedly linked to Alzheimer's disease pathology, the underlying mechanism is not known.

Methods: Here, we used ADNI-3 multishell diffusion magnetic resonance imaging data to separate the diffusion signal of the parenchyma from less hindered fluid pools within the white matter such as perivascular space fluid and fluid-filled cavities.

Results: We found that the source of the pathological increase of the mean diffusivity is the increased nonparenchymal fluid, often found in lacunes and perivascular spaces. In this cohort, the cognitive decline was significantly associated with the fluid increase and not with the microstructural changes of the white matter parenchyma itself. The white matter fluid increase was dominantly observed in the sagittal stratum and anterior thalamic radiation.

Discussion: These findings are positive steps toward understanding the pathophysiology of white matter alteration and its role in the cognitive decline.

© 2019 The Authors. Published by Elsevier Inc. on behalf of the Alzheimer's Association. This is an open access article under the CC BY-NC-ND license (http://creativecommons.org/licenses/by-nc-nd/4.0/).

Keywords: Preclinical AD; White matter alteration; White matter fluid; Nonparenchymal fluid

1. Introduction

White matter alteration is one of the hallmarks of Alzheimer's disease (AD) pathophysiology [1]. An emerging body of evidence suggests that white matter damage is among the earliest AD pathological changes, preceding cortical loss. Based on the two-hit vascular hypothesis [2], cerebrovascular alteration contributes to inefficient drainage of amyloid and increases the accumulation of amyloid-β, resulting in white matter damage [3]. A recent study showed even in the absence of age-related cerebrovascular disease, white matter alteration presented well before the onset of symptoms [4]. It is also believed that tau independently [5] contributes to white matter changes within AD defined regions. These findings highlight the significance of a technique that could map white matter health.

Increased mean diffusivity (MD) of the diffusion tensor imaging (DTI) is considered the neuroimaging signature of white matter degeneration in AD [6–19]. Increased MD was also shown to be a sensitive biomarker of prodromal

cerebrovascular health [20] or small vessel disease [21]. DTI, as an *in vivo*, noninvasive, and quantitative biomarker, is a valuable neuroimaging tool. However, the underlying mechanism for the increased MD is not completely understood, mainly because multiple tissue compartments with differing morphologies contribute to diffusion MRI signal, and DTI infers an average sum of all. Hence, DTI cannot determine the source of increased MD, which limits its utility in discovering the cause of the white matter alteration in AD and its efficacy as a monitoring biomarker for future treatments.

Multishell diffusion imaging, however, allows to decompose the diffusion signal into related tissue compartments [22–45] (see [46,47] for reviews), and therefore offers additional specificity to white matter composition. Here we utilized multishell diffusion images of ADNI-3 advanced neuroimaging data set to decipher the origin of the increased white matter MD associated with the cognitive decline.

2. Methods

2.1. Participants

Data used in the preparation of this article were obtained from the Alzheimer's Disease Neuroimaging Initiative (ADNI) database (http://adni.loni.usc.edu). Data from ADNI-3 cohort [48] were used, in which multishell diffusion MRI data are available. Data of 66 subjects with multishell diffusion MRI were downloaded from the ADNI database (http://adni.loni.usc.edu) [49]. To achieve a homogeneous patient group of preclinical AD, 3 subjects classified as AD were excluded. One cognitively normal (CN) subject was also excluded because of the young age (54-year-old). Subjects were divided into two groups of CN subjects ($N = 37$, 24 females) and patients with amnestic MCI ($N = 24$, 7 females). Average age of the CN ($M = 73.7$, $SD = 7.9$) and the amnestic MCI group ($M = 75.5$, $SD = 6.8$) was not statistically different ($t(59) = 0.93$, $P = .36$). The MCI group consists of patients with early cognitive decline based on Clinical Dementia Rating (CDR), Mini-Mental State Examination and Montreal Cognitive Assessment: (CDR(memory) = 0.36 ± 0.27, CDR(global) = 0.34 ± 0.24, Mini-Mental State Examination = 27.75 ± 2.63, Montreal Cognitive Assessment = 24 ± 3).

2.2. Data acquisition

All ADNI-3 images used in this study were acquired using Siemens Prisma or Prisma Fit 3T scanner (Siemens Healthcare, Erlangen, Germany), on six different sites, using a standardized diffusion MRI sequence [50]. Diffusion MRI data were acquired using the following parameters: 2D echoplanar axial imaging, with sliced thickness of 2 mm, in-plane resolution of 2 mm^2 (matrix size of 1044 x 1044), flip angle of 90°, TE = 71 ms, TR = 3.4 s, 126 diffusion-encoding images with three b-values (6 directions for b-value = 500 s/mm^2, 48 directions for b-value = 1000 s/mm^2, 60 directions for b-value = 2000 s/mm^2), with 13 non–diffusion-weighted images.

2.3. Investigating the source of the MD change

A tensor-based model (DTI) was first used to compare MD measures between groups. Then a bitensor model was used to extract three parameters that could contribute to the observed MD change, namely diffusivity of the parenchyma, diffusivity of the nonparenchymal fluid (e.g., fluid in lacunes and perivascular spaces), and relative volume of the nonparenchymal fluid. Note that the value related to the amount of fluid within the voxel is not the absolute volume fraction of the fluid, rather is the signal fraction of the diffusion signal associated with the fluid (myelin and cell membrane that are made of lipids and proteins do not contribute to the magnitude of the MRI signal).

2.4. Data processing

Raw images were converted to *nifti* file format using *dcm2nii* [51]. Diffusion MRI were corrected for eddy current distortion and for involuntary movement, using FSL TOPUP and EDDY tools [52,53]. DTI and a bitensor model were fitted to diffusion data using Quantitative Imaging Toolkit [54], as described in the study by Sepehrband et al [55]. The signal fraction that was fitted into a fast diffusing compartment (nonparenchymal fluid) was extracted as white matter fluid signal (WFS). Data were analyzed using Quantitative Imaging Toolkit to examine diffusion tensor parameters in deep white matter, as defined by the Johns Hopkins University (JHU) white matter atlas [56]. The JHU regions were segmented in each scan using an automated atlas-based approach described in the study by Cabeen et al. [57], in which deformable tensor-based registration using DTI toolkit [58] was used to align the subject data to the Illinois Institute of Technology diffusion tensor template [59], and subsequently to transform the JHU atlas regions to the subject data and compute the average of each diffusion tensor parameter with each JHU region. The native space T1-weighted MRI images were used to measure estimated total intracranial volume (eTIV) and hippocampal (HC) volume using the FreeSurfer software [60], as described in the study by Sepehrband et al [61]. In addition, volume of regions with white matter hyperintensities were measured using Lesion Mapper toolkit [62] and were compared between groups, but no significant difference was observed ($P = .7$).

2.5. Statistical analysis

We used a generalized linear model to investigate the association between WFS and cognitive stage using an ordinary least square fitting routine, implemented with the statsmodels.OLS module in Python 3.5.3 (StatsModels version 0.8.0— other Python packages that were used are Pandas version 0.20.3 and NumPy version 1.13.1). Median values of each region were used to remove the effect of imperfect boundary selection in periventricular areas. Measures from bilateral regions were averaged. Multiple regressions were fitted to regional values, one region at a time. For every instance, sex,

eTIV, HC volume, and age were included as covariates. The Benjamini–Hochberg procedure with a false discovery rate of 0.05 was used to correct for multiple comparisons. Statistical analysis was performed first on the MD values from DTI. Then WFS, MD of white matter parenchyma, and MD of the nonparenchymal fluid from bitensor model were analyzed.

3. Results

Increased global WFS was significantly associated with cognitive decline ($b = 0.002$, $t(56) = 4.3$, $P < .001$); controlled for age, sex, eTIV, and HC volume (Fig. 1). The effect size was 1.61 times larger than the association between HC volume decrease and CDR ($b = -261.75$, $t(55) = -2.03$, $P = .047$). Regional MD values, as derived by DTI, were significantly different between studied groups (MCI > CN) in multiple regions: thalamic radiation, fronto-occipital and longitudinal fasciculi, sagittal stratum and corticospinal, cingulum, fornix, and corpus callosum tracts. However, when fluid and parenchyma were separated, parenchymal MD was not different between groups. WFS of these regions were significantly different across groups (MCI > CN). No significant difference in the MD values of the nonparenchymal fluid was observed.

The cognitively impaired group showed significantly increased WFS compared with the CN group, in two of the aforementioned white matter regions, even after DTI-derived MD was included as covariate (Fig. 2): sagittal stratum ($b = 0.003$, $t(55) = 3.24$, $P < .01$) and anterior thalamic radiation ($b = 0.034$, $t(55) = 3.19$, $P < .05$). WFS increased with age in both groups across all white matter regions. Note that WFS difference of the sagittal stratum was higher in earlier ages (i.e., white matter alteration of the MCI group started in younger ages).

4. Discussion

We used multishell diffusion MRI to uncover the source of highly reproduced white matter increased MD in cognitive decline. We found that the white matter diffusion MRI signal change is mainly related to increased amount of fluid within the white matter, and not the white matter parenchyma itself. The increased fluid was dominantly observed in the anterior thalamic radiation and sagittal stratum regions. The amount of nonparenchymal white matter fluid in these regions was significantly higher in the amnestic MCI group than in CN group and was significantly associated with cognitive decline.

These findings are positive steps toward understanding the pathophysiology of white matter alteration and its role in the cognitive decline. Multishell diffusion MRI offers additional specificity compared with DTI, which could enable targeting, therapeutic planning, and disease monitoring. DTI-derived measures were often considered as measures of white matter integrity [6–19]; however, the pathophysiology of the white matter integrity alteration is hidden to DTI, and the changes are often interpreted as demyelination and axonal loss. Our results suggest that increased nonparenchymal fluid, such as increase of the perivascular space fluid and fluid-filled cavities, dominates the observed microscopic changes. Increased white matter fluid may precede white matter parenchymal degeneration as we did not observe any parenchymal microstructural changes in the studied amnestic MCI group.

We used a bitensor model to separate WFS from parenchymal signal, which we recently used to study the contribution of the perivascular space fluid on DTI measures [55]. Given that in this study, the entire white matter regions were explored, no assumption regarding the underlying source of the WFS is made. Although these changes could relate to perivascular space alteration [63,64], other pathological sources such as changes in interstitial fluid and lacunar infarct could also result in the accumulation of nonparenchymal white matter fluid [65–67]. Alteration of the vascular integrity could also affect the accumulation of nonparenchymal fluid.

With the assumption of the presence of a free water compartment with constant diffusion within the white matter, a recent diffusion study showed that the amount of the
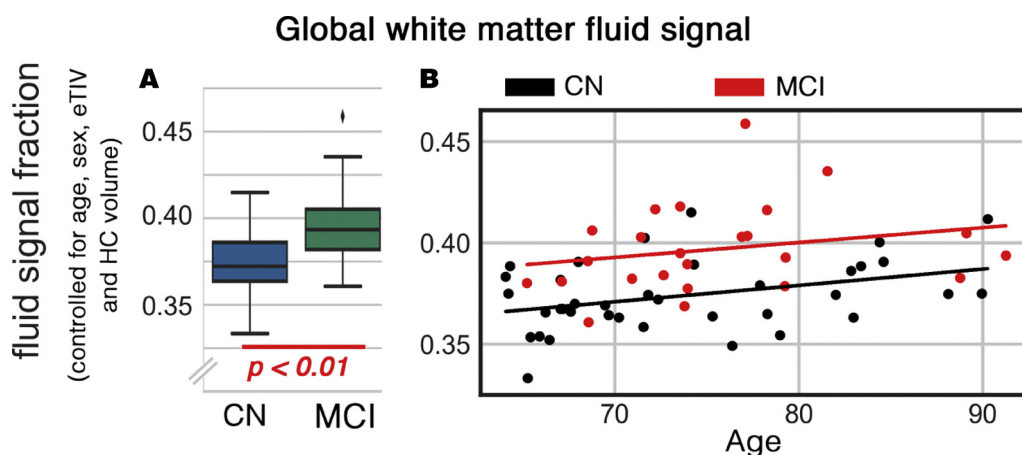

Fig. 1. Global white matter fluid signal (WFS) difference between cognitively normal (CN) and mild cognitively impaired (MCI) groups. (A) Mean global difference between CN and MCI, controlled for age, sex, eTIV, and the hippocampal (HC) volume. (B) The WFS changes as functions of cognitive state and age are demonstrated.
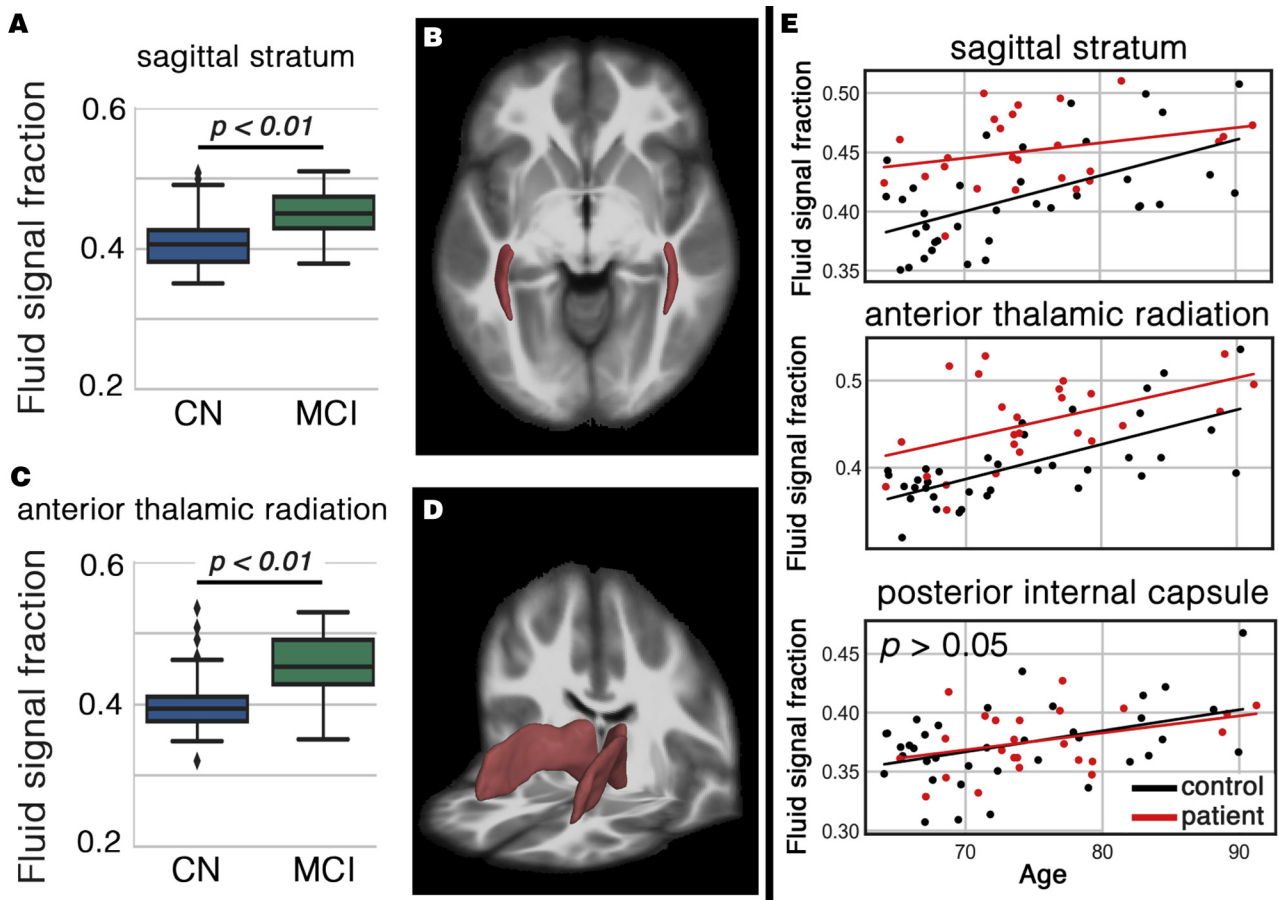
Fig. 2. White matter regions with significant higher white matter fluid signal (WFS) in cognitively impaired subjects. A shows the increased WFS in sagittal stratum. Sagittal stratum area is illustrated in B. Scatter plots C and D are related to the anterior thalamic area. Last column (E) shows the WFS of both groups as a function of age. Posterior internal capsule included as an example with no statistical difference to appreciate the extent of change in the affected white matter regions.

free water compartment is a sensitive marker of preclinical AD [68]. More recently, Dumont et al. showed that the free water compartment differentiates MCI from AD [69]. Our results corroborate these findings. However, unlike these studies, we did not use a fixed, free diffusing model for nonparenchymal fluid because of physiological and pathological factors that could affect the diffusivity of this compartment. Methodological details of dual-compartment modeling of diffusion MRI is presented in the study by Sepehrband et al [55].

In this study, we observed increase in diffusivity of the nonparenchymal fluid with age, but not between groups. Accumulation of toxic substances in extracellular, interstitial, cerebrospinal, and perivascular space fluids is expected to affect the composition of the fluid [63,67]. Such a compositional change could affect, most likely to a small degree, the diffusivity of the fluid in these regions. We speculate that a larger sample size and more advanced statistical approaches are required to capture such a subtle change.

Recently many studies claimed that the increased white matter fluid in AD might be secondary to vascular changes

[2,70], such as pericyte degeneration [71] and blood-brain barrier breakdown [72,73]; however, its temporal association with other AD markers is unknown. In sagittal stratum and anterior thalamic radiation, the WFS between-group differences were smaller in the older subjects, suggesting that the WFS may have reached or approached a plateau. In addition, the large WFS difference of the sagittal stratum in younger patients suggests that this region may be vulnerable to early-stage changes. Such accelerated and spatially differentiated white matter fluid increase demands further investigations.

Acknowledgments

RESEARCH IN CONTEXT

1. Systematic review: The authors reviewed the literature using conventional approaches such as searching PubMed repository. While increased mean diffusivity of the white matter has been repeatedly linked to Alzheimer's disease pathology, the underlying mechanism is not known.

2. Interpretation: We found that the source of the pathological increase of the mean diffusivity is the increased nonparenchymal fluid, often found in lacunes and perivascular spaces. The white matter fluid increase was dominantly observed in the sagittal striatum and anterior thalamic radiation.

3. Future directions: Such mechanistic understanding of the pathological signal change could enable treatment monitoring through noninvasive neuroimaging techniques. Future focuses on the longitudinal alteration of the white matter fluid could lead to better understanding of the early-stage changes of the AD pathology.

References

[1] Brun A, Englund E. A white matter disorder in dementia of the Alzheimer type: A pathoanatomical study. Ann Neurol 1986;19:253–62.

[2] Zlokovic BV. Neurovascular pathways to neurodegeneration in Alzheimer's disease and other disorders. Nat Rev Neurosci 2011;12:723–38.

[3] Iturria-Medina Y, Sotero RC, Toussaint PJ, Mateos-Pérez JM, Evans AC, Weiner MW, et al. Early role of vascular dysregulation on late-onset Alzheimer's disease based on multifactorial data-driven analysis. Nat Commun 2016;7:11934.

[4] Araque Caballero MÁ, Suárez-Calvet M, Duering M, Franzmeier N, Benzinger T, Fagan AM, et al. White matter diffusion alterations precede symptom onset in autosomal dominant Alzheimer's disease. Brain 2018;141:3065–80.

[5] Strain JF, Smith RX, Beaumont H, Roe CM, Gordon BA, Mishra S, et al. Loss of white matter integrity reflects tau accumulation in Alzheimer disease defined regions. Neurology 2018;91:e313–8.

[6] Kantarci K, Schwarz CG, Reid RI, Przybelski SA, Lesnick TG, Zuk SM, et al. White matter integrity determined with diffusion tensor imaging in older adults without dementia: Influence of amyloid load and neurodegeneration. JAMA Neurol 2014;71:1547–54.

[7] Kantarci K, Murray ME, Schwarz CG, Reid RI, Przybelski SA, Lesnick T, et al. White-matter integrity on DTI and the pathologic staging of Alzheimer's disease. Neurobiol Aging 2017;56:172–9.

[8] Wolf D, Fischer FU, Scheurich A, Fellgiebel A. Non-linear association between cerebral amyloid deposition and white matter microstructure in cognitively healthy older adults. J Alzheimers Dis 2015;47:117–27.

[9] Agosta F, Pievani M, Sala S, Geroldi C, Galluzzi S, Frisoni GB, et al. White matter damage in Alzheimer disease and its relationship to gray matter atrophy. Radiology 2011;258:853–63.

[10] Mayo CD, Mazerolle EL, Ritchie L, Fisk JD, Gawryluk JR. Longitudinal changes in microstructural white matter metrics in Alzheimer's disease. Neuroimage Clin 2017;13:330–8.

[11] Nir TM, Jahanshad N, Villalon-Reina JE, Toga AW, Jack CR, Weiner MW, et al. Effectiveness of regional DTI measures in distinguishing Alzheimer's disease, MCI, and normal aging. Neuroimage Clin 2013;3:180–95.

[12] Acosta-Cabronero J, Nestor PJ. Diffusion tensor imaging in Alzheimer's disease: Insights into the limbic-diencephalic network and methodological considerations. Front Aging Neurosci 2014;6:1–21.

[13] Cavedo E, Lista S, Rojkova K, Chiesa PA, Houot M, Brueggen K, et al. Disrupted white matter structural networks in healthy older adult APOE ε4 carriers–An international multicenter DTI study. Neuroscience 2017;357:119–33.

[14] Fellgiebel A, Wille P, Müller MJ, Winterer G, Scheurich A, Vucurevic G, et al. Ultrastructural hippocampal and white matter alterations in mild cognitive impairment: A diffusion tensor imaging study. Dement Geriatr Cogn Disord 2004;18:101–8.

[15] Naggara O, Oppenheim C, Rieu D, Raoux N, Rodrigo S, Dalla Barba G, et al. Diffusion tensor imaging in early Alzheimer's disease. Psychiatry Res 2006;146:243–9.

[16] Choi SJ, Lim KO, Monteiro I, Reisberg B. Diffusion tensor imaging of frontal white matter microstructure in early Alzheimer's disease: A preliminary study. J Geriatr Psychiatry Neurol 2005;18:12–9.

[17] Zhang Y, Schuff N, Jahng G-H, Bayne W, Mori S, Schad L, et al. Diffusion tensor imaging of cingulum fibers in mild cognitive impairment and Alzheimer disease. Neurology 2007;68:13–9.

[18] Zhang Y, Schuff N, Du A-T, Rosen HJ, Kramer JH, Gorno-Tempini ML, et al. White matter damage in frontotemporal dementia and Alzheimer's disease measured by diffusion MRI. Brain 2009;132:2579–92.

[19] Amlien IK, Fjell AM. Diffusion tensor imaging of white matter degeneration in Alzheimer's disease and mild cognitive impairment. Neuroscience 2014;276:206–15.

[20] Vemuri P, Lesnick TG, Przybelski SA, Graff-Radford J, Reid RI, Lowe VJ, et al. Development of a cerebrovascular MRI biomarker for cognitive aging. Ann Neurol 2018;84:705–16.

[21] Baykara E, Gesierich B, Adam R, Tuladhar AM, Biesbroek JM, Koek HL, et al. A novel imaging marker for small vessel disease based on skeletonization of white matter tracts and diffusion histograms. Ann Neurol 2016;80:581–92.

[22] Sepehrband F, O'Brien K, Barth M. A time-efficient acquisition protocol for multipurpose diffusion-weighted microstructural imaging at 7 Tesla. Magn Reson Med 2017;78:2170–84.

[23] Burcaw LM, Fieremans E, Novikov DS. Mesoscopic structure of neuronal tracts from time-dependent diffusion. Neuroimage 2015; 114:18–37.

[24] Tournier JD, Yeh CH, Calamante F, Cho KH, Connelly A, Lin CP. Resolving crossing fibres using constrained spherical deconvolution: Validation using diffusion-weighted imaging phantom data. Neuroimage 2008;42:617–25.

[25] Assaf Y, Blumenfeld-Katzir T, Yovel Y, Basser PJ. AxCaliber: A method for measuring axon diameter distribution from diffusion MRI. Magn Reson Med 2008;59:1347–54.

[26] Wedeen VJ, Wang RP, Schmahmann JD, Benner T, Tseng WYI, Dai G, et al. Diffusion spectrum magnetic resonance imaging (DSI) tractography of crossing fibers. Neuroimage 2008;41:1267–77.

[27] Assaf Y, Pasternak O. Diffusion tensor imaging (DTI)-based white matter mapping in brain research: A review. J Mol Neurosci 2008; 34:51–61.

[28] Jespersen SN, Kroenke CD, Østergaard L, Ackerman JJH, Yablonskiy DA. Modeling dendrite density from magnetic resonance diffusion measurements. Neuroimage 2007;34:1473–86.

[29] Descoteaux M, Angelino E, Fitzgibbons S, Deriche R. Regularized, fast, and robust analytical Q-ball imaging. Magn Reson Med 2007; 58:497–510.

[30] Alexander AL, Lee JE, Lazar M, Field AS. Diffusion tensor imaging of the brain. Neurotherapeutics 2007;4:316–29.

[31] Hassan MK, ul-Haq M, Amin M, Tahirullah, Nawaz A, Ullah H. Association between baseline parameters and end of treatment response to combination of conventional interferon & ribavirin in patients with chronic hepatitis C. J Postgrad Med Inst 2014;28:149–53.

[32] Sukstanskii AL, Yablonskiy DA, Ackerman JJH. Effects of permeable boundaries on the diffusion-attenuated MR signal: Insights from a one-dimensional model. J Magn Reson 2004;170:56–66.

[33] Pierpaoli C, Jones DK. Removing CSF contamination in brain DT-MRIs by using a two-compartment tensor model. Int Soc Magn Reson Med Meet 2004;c:1215.

[34] Sepehrband F, Clark KA, Ullmann JFP, Kurniawan ND, Leanage G, Reutens DC, et al. Brain tissue compartment density estimated using diffusion-weighted MRI yields tissue parameters consistent with histology. Hum Brain Mapp 2015;36:3687–702.

[35] Sundgren PC, Dong Q, Gómez-Hassan D, Mukherji SK, Maly P, Welsh R. Diffusion tensor imaging of the brain: Review of clinical applications. Neuroradiology 2004;46:339–50.

[36] Horsfield MA, Jones DK. Applications of diffusion-weighted and diffusion tensor MRI to white matter diseases-A review. NMR Biomed 2002;15:570–7.

[37] Alexander AL, Hasan KM, Lazar M, Tsuruda JS, Parker DL. Analysis of partial volume effects in diffusion-tensor MRI. Magn Reson Med 2001;45:770–80.

[38] Le Bihan D, Mangin JF, Poupon C, Clark CA, Pappata S, Molko N, et al. Diffusion tensor imaging: Concepts and applications. J Magn Reson Imaging 2001;13:534–46.

[39] Novikov DS, Fieremans E, Jensen JH, Helpern JA. Characterizing microstructure of living tissues with time-dependent diffusion. Proc Natl Acad Sci 2012;111:5088–93.

[40] Panagiotaki E, Walker-Samuel S, Siow B, Johnson SP, Rajkumar V, Pedley RB, et al. Noninvasive quantification of solid tumor microstructure using VERDICT MRI. Cancer Res 2014; 74:1902–12.

[41] Zhu D, Li K, Faraco CC, Deng F, Zhang D, Guo L, et al. Optimization of functional brain ROIs via maximization of consistency of structural connectivity profiles. Neuroimage 2012;59:1382–93.

[42] Wang Y, Wang Q, Haldar JP, Yeh FC, Xie M, Sun P, et al. Quantification of increased cellularity during inflammatory demyelination. Brain 2011;134:3587–98.

[43] Fieremans E, Jensen JH, Helpern JA. White matter characterization with diffusional kurtosis imaging. Neuroimage 2011; 58:177–88.

[44] Alexander DC, Hubbard PL, Hall MG, Moore EA, Ptito M, Parker GJM, et al. Orientationally invariant indices of axon diameter and density from diffusion MRI. Neuroimage 2010;52:1374–89.

[45] Jespersen SN, Bjarkam CR, Nyengaard JR, Chakravarty MM, Hansen B, Vosegaard T, et al. Neurite density from magnetic resonance diffusion measurements at ultrahigh field: Comparison with light microscopy and electron microscopy. Neuroimage 2010; 49:205–16.

[46] Novikov DS, Fieremans E, Jespersen SN, Kiselev VG. Quantifying brain microstructure with diffusion MRI: Theory and parameter estimation. NMR Biomed 2016;0:e3998.

[47] Alexander DC, Dyrby TB, Nilsson M, Zhang H. Imaging brain microstructure with diffusion MRI: Practicality and applications. NMR Biomed 2019;32:e3841.

[48] Weiner MW, Veitch DP, Aisen PS, Beckett LA, Cairns NJ, Green RC, et al. The Alzheimer's Disease Neuroimaging Initiative 3: Continued innovation for clinical trial improvement. Alzheimers Dement 2017; 13:561–71.

[49] Toga AW, Crawford KL. The informatics core of the Alzheimer's disease neuroimaging initiative. Alzheimers Dement 2010;6:247–56.

[50] Wyman BT, Harvey DJ, Crawford K, Bernstein MA, Carmichael O, Cole PE, et al. Standardization of analysis sets for reporting results from ADNI MRI data. Alzheimers Dement 2013;9:332–7.

[51] Li X, Morgan PS, Ashburner J, Smith J, Rorden C. The first step for neuroimaging data analysis: DICOM to NIfTI conversion. J Neurosci Methods 2016;264:47–56.

[52] Andersson JLR, Skare S, Ashburner J. How to correct susceptibility distortions in spin-echo echo-planar images: Application to diffusion tensor imaging. Neuroimage 2003;20:870–88.

[53] Andersson JLR, Xu J, Yacoub E, Auerbach E, Moeller S, Ugurbil K. A comprehensive Gaussian process framework for correcting distortions and movements in diffusion images. Jt Annu Meet Ismrm-esmrmb 2012;20:2426.

[54] Cabeen RP, Laidlaw DH, Toga AW. Quantitative imaging toolkit: Software for interactive 3D visualization, data exploration, and computational analysis of neuroimaging datasets. Proceedings of the International Society for Magnetic Resonance in Medicine (ISMRM) 2018:2854.

[55] Sepehrband F, Cabeen RP, Choupan J, Barisano G, Law M, Toga AW; Alzheimers Disease Neuroimaging Initiative, Perivascular space fluid contributes to diffusion tensor imaging changes in white matter. BioRxiv 2019:395012.

[56] Mori S, Oishi K, Jiang H, Jiang L, Li X, Akhter K, et al. Stereotaxic white matter atlas based on diffusion tensor imaging in an ICBM template. Neuroimage 2008;40:570–82.

[57] Cabeen RP, Bastin ME, Laidlaw DH. A Comparative evaluation of voxel-based spatial mapping in diffusion tensor imaging. Neuroimage 2017;146:100–12.

[58] Zhang H, Yushkevich PA, Alexander DC, Gee JC. Deformable registration of diffusion tensor MR images with explicit orientation optimization. Med Image Anal 2006;10:764–85.

[59] Zhang S, Peng H, Dawe RJ, Arfanakis K. Enhanced ICBM diffusion tensor template of the human brain. Neuroimage 2011;54:974–84.

[60] Fischl B. Freesurfer. Neuroimage 2012;62:774–81.

[61] Sepehrband F, Lynch KM, Cabeen RP, Gonzalez-Zacarias C, Zhao L, D'Arcy M, et al. Neuroanatomical morphometric characterization of sex differences in youth using statistical learning. Neuroimage 2018; 172:217–27.

[62] Wetter NC, Hubbard EA, Motl RW, Sutton BP. Fully automated open-source lesion mapping of T2-FLAIR images with FSL correlates with clinical disability in MS. Brain Behav 2016;6:1–9.

[63] Park L, Uekawa K, Garcia-Bonilla L, Koizumi K, Murphy M, Pistik R, et al. Brain perivascular macrophages initiate the neurovascular dysfunction of Alzheimer abeta peptides. Circ Res 2017;121:258–69.

[64] Bakker ENTP, Bacskai BJ, Arbel-Ornath M, Aldea R, Bedussi B, Morris AWJ, et al. Lymphatic clearance of the brain: Perivascular, paravascular and significance for neurodegenerative diseases. Cell Mol Neurobiol 2016;36.

[65] Gold G, Kövari E, Herrmann FR, Canuto A, Hof PR, Michel J-P, et al. Cognitive consequences of thalamic, basal ganglia, and deep white matter lacunes in brain aging and dementia. Stroke 2005;36:1184–8.

[66] Wardlaw JM, Smith EE, Biessels GJ, Cordonnier C, Fazekas F, Frayne R, et al. Neuroimaging standards for research into small vessel disease and its contribution to ageing and neurodegeneration. Lancet Neurol 2013;12:822–38.

[67] Rasmussen MK, Mestre H, Nedergaard M. The glymphatic pathway in neurological disorders. Lancet Neurol 2018;17:1016–24.

[68] Hoy AR, Ly M, Carlsson CM, Okonkwo OC, Zetterberg H, Blennow K, et al. Microstructural white matter alterations in preclinical Alzheimer's disease detected using free water elimination diffusion tensor imaging. PLoS One 2017;12:1–21.

[69] Dumont M, Roy M, Jodoin P-M, Morency FC, Houde J-C, Xie Z, et al. Free water in white matter differentiates MCI and AD from control subjects. BioRxiv 2019:537092.

[70] Sweeney MD, Kisler K, Montagne A, Toga AW, Zlokovic BV. The role of brain vasculature in neurodegenerative disorders. Nat Neurosci 2018;21:1318–31.

[71] Montagne A, Nikolakopoulou AM, Zhao Z, Sagare AP, Si G, Lazic D, et al. Pericyte degeneration causes white matter dysfunction in the mouse central nervous system. Nat Med 2018;24:326.

[72] Nation DA, Sweeney MD, Montagne A, Sagare AP, D'Orazio LM, Pachicano M, et al. Blood–brain barrier breakdown is an early biomarker of human cognitive dysfunction. Nat Med 2019;25:270–6.

[73] Sweeney MD, Sagare AP, Zlokovic BV. Blood–brain barrier breakdown in Alzheimer disease and other neurodegenerative disorders. Nat Rev Neurol 2018;14:133.